Cell Biochem Biophys (2015) 73:59–64
DOI 10.1007/s12013-015-0570-3

ORIGINAL PAPER

CT Features and Pathological Correlation of Primitive Neuroectodermal Tumor of the Kidney

Junqiang Dong · Jingjing Xing · Hangsha Hang Limbu · Songwei Yue · Lei Su · Dandan Zhang · Jianbo Gao

Published online: 8 February 2015
© Springer Science+Business Media New York 2015

Abstract The purpose of the study was to analyze the computed tomography (CT) findings of primitive neuroectodermal tumor (PNET) of the kidney and correlate them pathologically. Ten cases of pathologically confirmed renal PNET were collected and retrospectively reviewed. The CT features that were analyzed include tumor size, shape, margins, density, nature of enhancement, presence of thrombosis, and metastasis, etc. These parameters were correlated with pathological findings and combined with literature review. The median age of the patients was 30 years. CT images showed solitary, large, ill-defined, irregular, or lobulated heterogeneous mass. Invasive growth toward the renal cortex and pelvis with renal cortical interruptions were seen in eight cases with one case exhibiting invasion that extended beyond the renal capsule with soft tissue seen in the perirenal fat pace. The tumors were confined to the kidney contour with enlargement of kidney in six of the cases. Cystic changes with mural nodules were detected in three cases. Eight cases showed persistent moderate enhancement during the nephrographic phase. Irregular septum-like structures were seen in four cases. Thrombosis was detected in eight cases. Lymph node metastasis was detected in eight cases with bilateral lung metastasis in two and bone metastasis in one. Renal PNET is a rare highly aggressive disease affecting younger people. It should be considered as a strong differential when well confined, yet large tumors that cause enlargement of the kidney are seen and also when tumors expressing cystic changes along with mural nodules are seen. Although renal PNET has certain other characteristic CT features, pathological and immunohistochemistry report must also be sought for definitive diagnosis.

Keywords Renal neoplasms · Primitive neuroectodermal tumor · Tomography · X-ray computed

Introduction

PNETs are a rare, highly aggressive group of small round cell tumors predominantly of neuroectodermal origin outside the central and sympathetic nervous systems. These neoplasms are commonly located in the soft tissues of thoracopulmonary region, paraspinal region, and limbs. PNETs represent less than 1 % of renal tumors [1]. Very few cases of renal PNET have been reported in literature with focus on radiological findings and hence there is a lack of awareness of its clinical and scan findings that has led to frequent misdiagnosis. In view of this, the CT features were critically studied in a retrospective analysis of pathologically confirmed renal PNETs in our hospital. Detailed literature review helped to further explore the disease.

Materials and Methods

Clinical and CT data from 10 cases of pathologically confirmed renal PNET patients, who visited the hospital

Junqiang Dong and Jingjing Xing have equally contributed to this paper and should be regarded as co-first author.

J. Dong · J. Xing · H. H. Limbu · S. Yue · L. Su · J. Gao (✉)
Department of Radiology, The 1st Affiliated Hospital of Zhengzhou University, No.1 The Eastern Jian She Road, Zhengzhou 450052, China
e-mail: jianbogao@yahoo.com

D. Zhang
Department of Pathology, The 1st Affiliated Hospital of Zhengzhou University, No.1 The Eastern Jian She Road, Zhengzhou 450052, China

between January 2011 and January 2014, were collected and retrospectively reviewed. An institutional review board exemption and a waiver for the requirement of a written informed consent were obtained to perform this retrospective study.

Eight cases were examined with GE Discovery 750 HD CT, and 2 with Toshiba 320 CT. The scanning parameters for the former machine were: tube voltage of 120 kV, automatic mA, pitch of 0.984, thickness of 5 mm; and the scanning parameters for the latter machine were: tube voltage of 120 kV, tube current of 350 mA, pitch of 0.813, thickness of 5 mm; increment reconstruction in both was 3 mm. The patients were in fasting condition for more than 6 h before the CT scan. First routine kidney scan was done which was followed by the contrast-enhanced scan. Intravenous bolus dose of contrast agent Iohexol (320 mgI/ml) was administered at a rate of 3.0–4.0 ml/s and a dose of 1.5 ml/kg. Contrast-enhanced CT scans were obtained 25 s after administration of contrast agent for corticomedullary phase and after 60 s for the nephrographic phase.

Two experienced radiologists reviewed the CT features of each of the unenhanced as well as enhanced images, which included location, shape, size, margin, density, necrotic and cystic changes, presence and extent of venous thrombosis, nature of enhancement, metastasis, etc. The CT features were compared with the findings of other literatures and detailed literature review was carried out.

For the histological studies, specimens were fixed in 10 % formalin, and tissues were prepared by the routine procedure. The paraffin-embedded preparations underwent routine hematoxylin-eosin stain and IHC examinations.

Results

Ten cases were documented aged between 19 and 78 years with a median age of 30 years. Male predominance was seen with 8 male cases and 2 female cases. Six cases complained of flank pain, 3 cases complained of hematuria, and 1 case complained of lower limb pain with weakness for a month. On physical examination, 6 cases had renal angle tenderness with palpation of renal mass in 2 of them and the remaining 4 cases had normal abdominal findings.

Important CT features of the ten cases are summarized in Table 1. CT images showed solitary large mass in all 10 cases with maximum diameter of 6.2–21.6 cm. Six of the tumors were located in the right kidney and four in the left kidney. Two were lobular in shape and eight were irregular in shape. The margins of the tumor were unclear, and eight of them showed invasive growth invading the renal cortex and pelvis with renal cortical interruptions (Fig. 1). One of the cases had an invasion extending beyond the renal capsule

Table 1 CT features of 10 cases of renal PNET

Patients no.	Location	Size (cm)	Border	Necrosis/cystic changes	Mural nodules	Calcification	Growth	Enhancement		Thrombosis		Metastasis	
								Corticomedullary phase	Nephrographic	Renal vein	IVC	Lymph nodes	Distant
1	R	7.2	III	+	+	+	Expansive	Mild	Moderate	−	−	+	Bone
2	R	9.8	III	−	−	−	Invasive	Mild	Mild	+	−	−	−
3	L	6.2	III	+	+	−	Invasive	Mild	Moderate	+	+	+	Lung
4	R	10.2	III	−	−	−	Invasive	Mild	Mild	+	−	−	−
5	L	7.8	III	−	−	−	Invasive	Mild	Moderate	+	+	+	−
6	L	9.7	III	−	−	−	Invasive	Mild	Moderate	+	+	+	−
7	R	8.6	III	+	−	−	Invasive	Mild	Moderate	+	+	+	−
8	R	8.1	III	+	−	−	Expansive	Mild	Moderate	−	−	+	−
9	L	9.2	III	+	+	−	Invasive	Mild	Moderate	+	+	+	Lung
10	R	21.6	III	+	−	−	Invasive	Mild	Moderate	+	+	+	−

with soft tissue seen in the perirenal fat space, combined with urethral and renal pelvis invasion with enlarged calyces and renal stones (Fig. 2). Six of the cases exhibited enlarged kidney with large tumor size but well confined within the kidney contour. Necrosis was seen in 3 cases and combined necrosis and cystic changes were seen in 3 cases of which visible mural nodules and cystic areas located around the tumor were seen in 3 cases. Patchy calcification was seen in one of the cases with mural nodules (Fig. 3). CT values of solid component averaged 44 HU, 58 HU, and 82 HU in unenhanced images, corticomedullary phase, and nephrographic phase, respectively. All cases showed mild heterogeneous enhancement during corticomedullary phase; 2 had persistent mild enhancement and 8 had persistent moderate enhancement during nephrographic phase with irregular septum-like structures seen in 4 cases (Fig. 4). Eight cases had renal vein thrombosis (Fig. 1b) of which 6 cases had extension of thrombus into the inferior vena cava (IVC) (Fig. 1c). Retroperitoneal lymph node metastasis was detected in 8 cases, bone metastasis was detected in 1 case in the cervical and thoracic vertebra, and bilateral lung metastasis was detected in 2 cases. Three cases had pleural effusion and 2 cases had ascites.

Histopathological slides revealed tumors comprising uniform population of small round cells, with deeply stained nuclei and mitotic figures observed frequently. The tumor cells were arranged into lobules by fibrous vascular septa and formed perivascular pseudorosettes and Homer-Wright-type rosettes (Fig. 5). IHC examination showed CD99 positive in all 10 cases, Vimentin and Syn positive in 8 of the cases, CD56 positive in 6 cases, NSE positive in 4 cases, and S-100 positive in 2 of the cases.

Discussion

PNETs are a rare group of small round cell tumor originating from neuroectoderm classified as central type (cPNET) and peripheral type (pPNET), with kidney as an uncommon site of origin [2, 3]. Though renal PNETs can occur at any age, it is more common in young people between 10 and 39 years of age, which accounts for around 75 % of the cases [4, 5] with a male predominance [6]. Consistent with this, 9 cases of our group were aged between 19 and 37 years with a male predominance. Patients of renal PNETs presented with non-specific clinical symptoms as first signs of disease with pain being the most frequent followed by hematuria, renal mass, and in few cases fever, weight loss, fatigue, and abdominal swelling [1]. The clinical features of our group were consistent with other literature findings.

PNETs are large in size with mean diameter greater than 5 cms [7]. CT imaging features include large, ill-defined, irregular, or lobular heterogeneous mass with multifocal or diffuse peripheral necrotic and cystic changes [8]. Demonstration of calcification in PNET is rare [9]. In this study, the tumors were solitary and the maximum diameter ranged from 6.2 to 21.6 cm. Multiple focal necrosis was seen in 3 cases and peripheral cystic degeneration with mural nodules was seen in 3 cases of which 1 demonstrated patchy calcification.

Contrast-enhanced scan of renal PNET presented with mild to moderate heterogenous enhancement during corticomedullary phase with persistent enhancement during the nephrographic phase [7]. Consistent with the literature, all the 10 cases showed mild heterogeneous enhancement during corticomedullary phase and 8 cases showed persistent moderate enhancement with 2 persistent mild enhancement during nephrographic phase. The tumor vasculature is rich, but due to the presence of dense tumor cells, there is slow clearance of contrast agent, leading to sustained mild to moderate enhancement. The heterogeneous enhancement of the mass may be explained by the formation of pseudorosette or Homer-Wright rosettes, surrounding the small blood vessels and fiber in the tumor cells [10], which is a characteristic feature of PNETs. 4

Fig. 1 Left renal PNET in a 19-year-old male. **a** Contrast-enhanced CT images during the corticomedullary phase show large tumor with ill-defined margin invading the renal cortex and pelvis, enlarging the kidney volume, but well confined within the kidney contour, cortical interruption is seen; **b**, **c** Contrast-enhanced CT images during the nephrographic phase show low-density filling defect in the left renal vein and inferior vena cava (*arrowheads*), pathologically confirmed to be thrombosis (**c**). A cystic tumor with an oval shaped mural nodule

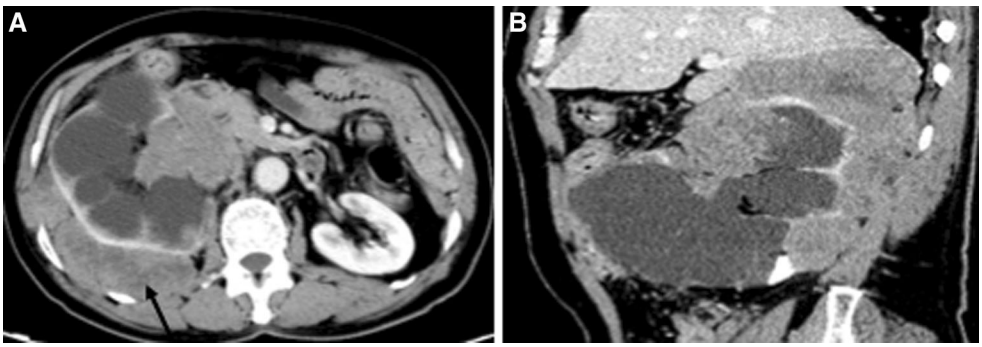

Fig. 2 Right renal PNET in a 78-year-old male (**a**), Contrast-enhanced CT image during nephrographic phase, shows perinephric fat tissue extension (*arrow*) (**b**), Contrast-enhanced sagittal CT image shows tumor breaking through the renal capsule and invading the perirenal fat space as well as invading the renal pelvis, with enlarged calyces and a visible renal stone

Fig. 3 Right renal PNET with cystic changes in a 26-year-old female (**a**, **b**), Contrast-enhanced coronal CT images during the corticomedullary and nephrographic phase respectively, showed two oval mural nodules with visible renal hilar lymph node metastasis (**c**), Non-contrast CT image shows the mural nodule with patchy calcification (*white arrow*)

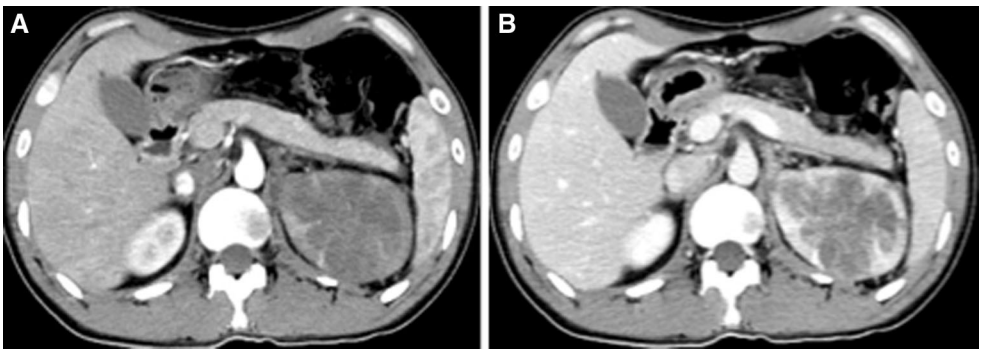

Fig. 4 Left renal PNET in 30-year-old male. Contrast-enhanced CT images showed that tumor has mild heterogeneous enhancement during corticomedullary phase (**a**) with persistent moderate enhancement during nephrographic phase (**b**), lower than the renal cortex and with irregular septum-like structures

cases also demonstrated the presence of irregular septa-like structures, a feature thought to be a characteristic CT finding of renal PNETs [7]. Microscopically, the intra tumoral nodules are separated by fibrovascular septa forming a mesh work or clusters and we believe these fibrovascular septa are responsible for the demonstration of irregular septa-like structures.

Renal PNETs are highly invasive and often without an envelope. They are prone to metastasis and invasion of surrounding organs and vasculature. Lymph node metastasis occurs most often, followed by lung, liver, and bone [5]. Consistent with the literature, in the study too we had 8 cases of peritoneal lymph node metastasis, 2 cases of lung metastasis, and 1 case of bone metastasis. The tumor commonly originates from the renal medulla and invades along the renal parenchyma extending outwards to the renal cortex, presenting as cortical interruptions that break through the renal capsule invading the perinephric fat space

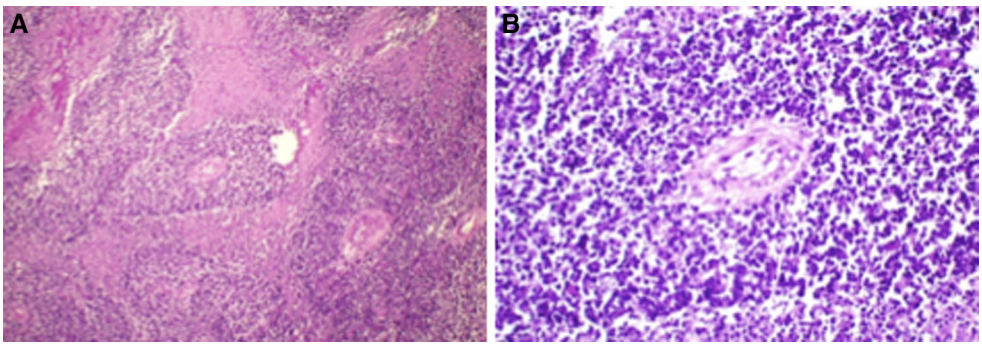

Fig. 5 Histopathological findings of biopsy in a 26-year-old female (HEx100 and HEx400 respectively) (**a**, **b**) showed small round cell tumor with Homer-Wright rosette formations

[11]. Such a presentation was seen in 1 case in the study. Almeida et al. [12] had reported one case where the mass broke into the hepatorenal space and invaded the right liver. PNET of the kidney is commonly observed with renal vein thrombosis frequently extending to the IVC [13]. In this study, 8 of the cases in the study had renal vein thrombosis, and 6 of them had thrombus extending to IVC. Thrombus is related to tumor growth and invasion depicting its highly malignant behavior. PNET's prognosis is poor, and combined with metastasis and venous thrombosis, it is even more [14].

After conducting an extensive review of all available literatures on the CT findings of renal PNET, the 10 cases studied brought forward two characteristic features which were not discussed in literature before. First, in this group, there were 6 cases of large tumor, increasing the volume of the kidney; however, they were well confined within the kidney contour. The reason for the tumor being well confined within the kidney contour maybe due to the renal medullary origin of the tumor inducing invasive and expansive growth centered around the renal cortex.

Second, mural nodules were detected in 3 of the cases of cystic degeneration, with the presence of patchy calcification in one of them. Presence of mural nodules in renal PNET has not been reported in literature before, and further review is required regarding its diagnostic value for PNET of the kidney.

The definitive diagnosis of PNET is based on the pathologic findings, assisted by IHC evaluation. The presence of Homer-Wright rosettes or IHC expression of at least two different neural markers renders the diagnosis of PNET [15]. Among the IHC markers CD99 has high specificity with Vimentin, Synaptophysin, NSE, CD56, S100 protein, etc. as other markers of neural differentiation associated with PNETs [16]. Consistent with the literature, Homer-Wright rosettes were detected in all the 10 cases histopathologically and CD99 was positive for all the cases with at least one additional neural marker positive for each case.

PNETs are highly aggressive and are often diagnosed late with poor prognosis. Metastasis is a very common finding even after complete removal of the tumor. Recent advances have shown that combination of surgery, radiation therapy, and chemotherapy has better outcomes [17], but correct early diagnosis is of utmost importance. CT imaging has been the choice of investigation for detecting the tumor and metastasis and an aid in deciding the course of treatment.

Based on the CT findings, renal carcinomas such as renal cell carcinoma (RCC), renal lymphoma, Wilms' tumor, renal pelvis carcinoma, etc. should be considered as differentials of PNET. RCCs are the most common tumors of the kidney mostly originating from the renal cortex. Unlike PNET, they present commonly in men over 40 years and are typically solid lesions, but large RCCs usually contain central necrosis or cystic change while PNETs have peripheral distribution. Contrast study of RCC shows variable enhancement but highly enhancing mass should be considered as RCC.

Renal lymphomas are common in elderly and are often bilateral. Multinodular masses of homogenous density are characteristic radiological findings of lymphoma. Renal invasion from contiguous retroperitoneal masses is a common finding. The renal arteries and vein are patent despite tumor invasion, unlike PNETs where renal vein thrombosis is often observed.

Wilms' tumor is common in children under 4 years of age, appearing as a large, spherical mass with well-defined rim of compressed normal renal parenchyma or a pseudocapsule surrounding it and medial displacement of the kidney. Contrast-enhanced image presents as hypodense mass surrounded by enhanced rim of normal parenchyma.

Renal pelvis carcinoma is common in elderly people presenting with painless hematuria. CT image shows mass typically of soft tissue density centered on the renal pelvis, ranging from small filling defects in size to large masses obliterating the renal sinus fat.

The present study has small number of patients and might not reflect the full imaging features of PNETs. Furthermore, due to its retrospective nature the differences in imaging techniques might have influenced the interpretation. Further studies with a larger number of patients are necessary for better understanding of the radiological features of the disease.

Renal PNET is a rare kidney tumor with poor prognosis. It should be considered as a strong differential when cystic changes with mural nodules and a large tumor enlarging the volume but well confined within the kidney are seen. Other features of renal PNET include ill-defined large heterogeneous mass showing infiltrative growth into the renal parenchyma with necrotic and cystic changes and contrast-enhanced scan showing persistent enhancement during the nephrographic phase commonly accompanied by venous thrombosis and metastasis.

Conflict of interest The author declares no conflict of interest.

References

1. Risi, E., Iacovelli, R., Altavilla, A., et al. (2013). Clinical and pathological features of primary neuroectodermal tumor/Ewing sarcoma of the kidney. *Urology, 82*, 382–386.
2. Parham, D. M., Roloson, G. J., Feely, M., et al. (2001). Primary malignant neuroepithelial tumors of the kidney: A clinicopathologic analysis of 146 adult and pediatric cases from the National Wilms' Tumor Study Group Pathology Center. *American Journal of Surgical Pathology, 25*, 133–146.
3. Lalwani, N., Prasad, S. R., Vikram, R., et al. (2011). Pediatric and adult primary sarcomas of the kidney: A cross-sectional imaging review. *Acta Radiologica, 52*, 448–457.
4. Ekram, T., Elsayes, K. M., Cohan, R. H., et al. (2008). Computed tomography and magnetic resonance features of renal Ewing sarcoma. *Acta Radiologica, 49*, 1085–1090.
5. Ellinger, J., Bastian, P. J., Hauser, S., et al. (2006). Primitive neuroectodermal tumor: Rare, highly aggressive differential diagnosis in urologic malignancies. *Urology, 68*, 257–262.
6. Zöllner, S., Dirksen, U., Jürgens, H., et al. (2013). Renal Ewing tumors. *Annals of Oncology, 24*, 2455–2461.
7. Qian, X., Kai, X., Shaodong, L., et al. (2013). Radiological and clinicopathological features of pPNET. *European Journal of Radiology, 82*, e888–e893.
8. Lee, H., Cho, J. Y., Kim, S. H., et al. (2009). Imaging findings of primitive neuroectodermal tumors of the kidney. *Journal of Computer Assisted Tomography, 33*, 882–886.
9. Li, X., Zhang, W., Song, T., et al. (2011). Primitive neuroectodermal tumor arising in the abdominopelvic region: CT features and pathology characteristics. *Abdominal Imaging, 36*, 590–595.
10. Murphey, M. D., Senchak, L. T., Mambalam, P. K., et al. (2013). From the radiologic pathology archives: Ewing sarcoma family of tumors: Radiologic-pathologic correlation. *Radiographics, 33*, 803–831.
11. Lazzara, B. M., Scalcione, L. R., Garnet, D. J., et al. (2012). Radiology-pathology conference: Primary perinephric and renal extraosseous Ewing's sarcoma. *Clinical Imaging, 36*, 77–79.
12. Almeida, M. F., Patnana, M., Korivi, B. R., et al. (2014). Ewing sarcoma of the kidney: A rare entity. *Case Reports in Radiology, 2014*, 283902.
13. Chu, W. C., Reznikov, B., Lee, E. Y., et al. (2008). Primitive neuroectodermal tumour (PNET) of the kidney: A rare renal tumour in adolescents with seemingly characteristic radiological features. *Pediatric Radiology, 38*, 1089–1094.
14. Rodriguez-Galindo, C., Marina, N. M., Fletcher, B. D., et al. (1997). Is primitive neuroectodermal tumor of the kidney a distinct entity? *Cancer, 79*, 2243–2250.
15. Ng, S. B., Sirrampalam, K., & Chuah, K. L. (2002). Primitive neuroectodermal tumours of the uterus: A case report with cytological correlation and review of the literature. *Pathology, 34*, 455–461.
16. Jimenez, R. E., Folpe, A. L., Lapham, R. L., et al. (2002). Primary Ewing's sarcoma/primitive neuroectodermal tumor of the kidney: A clinicopathologic and immunohistochemical analysis of 11 cases. *American Journal of Surgical Pathology, 26*, 320–327.
17. Ohgaki, K., Horiuchi, K., Mizutani, S., et al. (2010). Primary Ewing's sarcoma/primitive neuroectodermal tumor of the kidney that responded to low-dose chemotherapy with ifosfamide, etoposide, and doxorubicin. *International Journal of Clinical Oncology, 15*, 210–214.